On the Exactness of Rational Polynomial Chaos Formulation for the Uncertainty Quantification of Linear Circuits in the Frequency Domain

Paolo Manfredi and Stefano Grivet-Talocia

Abstract We discuss the general form of the transfer functions of linear lumped circuits. We show that an arbitrary transfer function defined on such circuits has a functional dependence on individual circuit parameters that is rational, with multilinear numerator and denominator. This result demonstrates that rational polynomial chaos expansions provide more suitable models than standard polynomial chaos for the uncertainty quantification of this class of circuits.

1 Introduction

The polynomial chaos expansion (PCE) method [1] has emerged in the macromodeling and model-order reduction communities because of the remarkable accuracy and efficiency in the uncertainty quantification by stochastic systems, including electric and electronic circuits [2]. Stochastic output variables of interest are approximated with a suitable polynomial model w.r.t. random input parameters, from which statistical information is inexpensively extracted. While the method was demonstrated to provide very high accuracy with a very limited expansion order in many application scenarios, the modeling of resonant and/or distributed circuits may require large orders and the accuracy of the calculated PCE coefficients may be deteriorated by the large variability of the outputs.

A rational polynomial chaos (RPC) model with tensor-product truncation was recently introduced [3] and was shown to provide better performance, compared to the conventional single PCE with total-degree truncation that is used in most engineering applications, specifically in electrical engineering [2]. In this work, we show that the general form of any transfer function defined for a linear lumped circuit is rational w.r.t. both frequency and element values. Specifically, both numerator and

Paolo Manfredi, Stefano Grivet-Talocia
Politecnico di Torino, Corso Duca degli Abruzzi 24, 10129 Torino (Italy), e-mail: paolo.manfredi@polito.it, stefano.grivet@polito.it

denominator are multi-linear functions of element values. We provide a rigorous and formal proof of this fundamental theoretical result that is somewhat well-known in electrical engineering [4], but unavailable in an unambiguous and explicit form. Thanks to the theoretical findings herein presented, we are able to show that the RPC model is exact and should be the method of choice for lumped circuits.

2 Rational Polynomial Chaos Expansion

Given an arbitrary transfer function, generically denoted with Z and defined on a linear lumped electrical circuit with d uncertain elements collected into vector $\boldsymbol{\xi} = (\xi_1, \ldots, \xi_d)$, its RPC model reads [3]

$$Z(s, \boldsymbol{\xi}) \approx \frac{\sum_{\ell=1}^{L} N_\ell(s)\varphi_\ell(\boldsymbol{\xi})}{1 + \sum_{\ell=2}^{L} D_\ell(s)\varphi_\ell(\boldsymbol{\xi})} \tag{1}$$

where s is the Laplace variable (complex frequency). In (1), the basis functions φ_ℓ are multivariate orthogonal polynomials in the uncertain variables $\boldsymbol{\xi}$, and the coefficients N_ℓ and D_ℓ are computed using a linearized and iteratively re-weighted regression. It was empirically shown [3] that, for the uncertainty quantification of electric circuits, the RPC (1) is more accurate than the standard PCE [2]. The purpose of this work is to provide a rigorous justification.

3 Transfer Functions of Linear Lumped Circuits

We review the basic modified nodal analysis (MNA) formulation [5] of lumped linear time-invariant (LTI) circuits with RGLC components. The main objective of this derivation is to reveal in explicit form the functional dependence on the individual circuit parameters of any transfer function that can be defined on such circuits.

3.1 Basic MNA Formulation for RGLC Circuits

Let us consider a lumped LTI P-port circuit with n nodes and b branches (one-port elements). The branches are split into b_R resistors with resistance R_k, b_G resistors with conductance G_k, b_L inductors with inductance L_k, and b_C capacitors with capacitance C_k, where k is an index identifying individual components. We distinguish between resistance-defined and conductance-defined resistors to allow additive variations of either parameter. In addition, the last $b_J = P$ branches are assumed to represent the P ports of the structure. We place ideal current sources J_k providing an excitation to the circuit, with the objective of characterizing the $P \times P$

impedance matrix $\boldsymbol{Z}(s)$ in the Laplace domain by computing the corresponding port voltages as outputs.

The branch voltage and current vectors $\boldsymbol{v}, \boldsymbol{i} \in \mathbb{R}^b$ are split according to element types as

$$\boldsymbol{v} = \left(\boldsymbol{v}_R^\mathsf{T}, \boldsymbol{v}_G^\mathsf{T}, \boldsymbol{v}_L^\mathsf{T}, \boldsymbol{v}_C^\mathsf{T}, \boldsymbol{v}_J^\mathsf{T}\right)^\mathsf{T}, \quad \boldsymbol{i} = \left(\boldsymbol{i}_R^\mathsf{T}, \boldsymbol{i}_G^\mathsf{T}, \boldsymbol{i}_L^\mathsf{T}, \boldsymbol{i}_C^\mathsf{T}, \boldsymbol{i}_J^\mathsf{T}\right)^\mathsf{T},$$

where $\boldsymbol{v}_\nu, \boldsymbol{i}_\nu \in \mathbb{R}^{b_\nu}$ for $\nu \in \{R, G, L, C, J\}$, and where the passive sign convention is used for each branch, including sources. The branch characteristic equations are collectively written for each class of components as

$$\boldsymbol{v}_R = \boldsymbol{R}\,\boldsymbol{i}_R \qquad \boldsymbol{R} = \mathrm{diag}(R_1, \ldots, R_{b_R}) \tag{2a}$$
$$\boldsymbol{i}_G = \boldsymbol{G}\,\boldsymbol{v}_G \qquad \boldsymbol{G} = \mathrm{diag}(G_1, \ldots, G_{b_G}) \tag{2b}$$
$$\boldsymbol{v}_L = \boldsymbol{L}\,\frac{d}{dt}\,\boldsymbol{i}_L \qquad \boldsymbol{L} = \mathrm{diag}(L_1, \ldots, L_{b_L}) \tag{2c}$$
$$\boldsymbol{i}_C = \boldsymbol{C}\,\frac{d}{dt}\,\boldsymbol{v}_C \qquad \boldsymbol{C} = \mathrm{diag}(C_1, \ldots, C_{b_C}) \tag{2d}$$
$$\boldsymbol{i}_J = -\boldsymbol{J} \qquad \boldsymbol{J} = (J_1, \ldots, J_{b_J})^\mathsf{T}. \tag{2e}$$

Note that the current J_k of each source is incident into its positive node.

Circuit connectivity is described by the (reduced) incidence matrix $\boldsymbol{A} \in \mathbb{R}^{n-1,b}$, with the n-th node serving as reference for the definition of the set of nodal voltages $\boldsymbol{e} \in \mathbb{R}^{n-1}$. The incidence matrix columns are partitioned according to the branch classes as

$$\boldsymbol{A} = \left(\boldsymbol{A}_R, \boldsymbol{A}_G, \boldsymbol{A}_L, \boldsymbol{A}_C, \boldsymbol{A}_J\right). \tag{3}$$

Combining Kirchhoff's current law (KCL) equations $\boldsymbol{A}\boldsymbol{i} = \boldsymbol{0}$ and Kirchhoff's voltage law (KVL) equations $\boldsymbol{v}_\nu = \boldsymbol{A}_\nu^\mathsf{T}\boldsymbol{e}$ for $\nu \in \{R, G, L, C, J\}$ with the characteristics (2), leads to the system of linear differential-algebraic equations

$$\boldsymbol{\mathcal{G}}\,\boldsymbol{x} + \boldsymbol{\mathcal{C}}\,\frac{d}{dt}\,\boldsymbol{x} = \boldsymbol{\mathcal{B}}\,\boldsymbol{u} \tag{4a}$$
$$\boldsymbol{y} = \boldsymbol{\mathcal{B}}^\mathsf{T}\,\boldsymbol{x}, \tag{4b}$$

which represents the standard MNA formulation. In (4), $\boldsymbol{u} = \boldsymbol{J}$ denotes the port currents, considered as inputs, $\boldsymbol{y} = \boldsymbol{v}_J$ denotes the corresponding port voltages, considered as outputs, vector $\boldsymbol{x} \in \mathbb{R}^m$, with $m = n - 1 + b_R + b_L$, collects the MNA variables $\boldsymbol{e}$, $\boldsymbol{i}_R$, $\boldsymbol{i}_L$, and

$$\boldsymbol{\mathcal{G}} = \begin{pmatrix} \boldsymbol{A}_G\boldsymbol{G}\boldsymbol{A}_G^\mathsf{T} & \boldsymbol{A}_R & \boldsymbol{A}_L \\ -\boldsymbol{A}_R^\mathsf{T} & \boldsymbol{R} & \boldsymbol{0} \\ -\boldsymbol{A}_L^\mathsf{T} & \boldsymbol{0} & \boldsymbol{0} \end{pmatrix}, \quad \boldsymbol{\mathcal{C}} = \begin{pmatrix} \boldsymbol{A}_C\boldsymbol{C}\boldsymbol{A}_C^\mathsf{T} & \boldsymbol{0} & \boldsymbol{0} \\ \boldsymbol{0} & \boldsymbol{0} & \boldsymbol{0} \\ \boldsymbol{0} & \boldsymbol{0} & \boldsymbol{L} \end{pmatrix}, \quad \boldsymbol{\mathcal{B}} = \begin{pmatrix} \boldsymbol{A}_J \\ \boldsymbol{0} \\ \boldsymbol{0} \end{pmatrix}. \tag{5}$$

Throughout this work, we denote with $\boldsymbol{0}$ an all-zero matrix or vector, whose size is inferred from the context.

The so-called *stamps* of the individual circuit elements in the MNA system (4) are now easily characterized. A straightforward derivation shows that

$$\boldsymbol{\mathcal{G}}(\boldsymbol{\theta}) = \boldsymbol{\mathcal{G}}_0 + \sum_{k=1}^{b_a} (\boldsymbol{p}_k \boldsymbol{p}_k^{\mathsf{T}})\, \theta_k, \quad \boldsymbol{\mathcal{C}}(\boldsymbol{\zeta}) = \sum_{k=1}^{b_d} (\boldsymbol{q}_k \boldsymbol{q}_k^{\mathsf{T}})\, \zeta_k, \tag{6}$$

where

- $b_a = b_R + b_G$ is the number of adynamic components with values collected in vector $\boldsymbol{\theta} \in \mathbb{R}^{b_a}$, having elements $\{\theta_k\}_{k=1}^{b_a} = \{R_k\}_{k=1}^{b_R} \cup \{G_k\}_{k=1}^{b_G}$;
- $b_d = b_L + b_C$ is the number of dynamic components with values collected in vector $\boldsymbol{\zeta} \in \mathbb{R}^{b_d}$, having elements $\{\zeta_k\}_{k=1}^{b_d} = \{L_k\}_{k=1}^{b_L} \cup \{C_k\}_{k=1}^{b_C}$;
- the constant vectors $\boldsymbol{p}_k \in \mathbb{R}^m$ collect the sets $\{\boldsymbol{p}_k\}_{k=1}^{b_a} = \{\boldsymbol{r}_k\}_{k=1}^{b_R} \cup \{\boldsymbol{g}_k\}_{k=1}^{b_G}$ individually defined as $\boldsymbol{r}_k = \left(\boldsymbol{0}, \boldsymbol{1}_{b_R,k}^{\mathsf{T}}, \boldsymbol{0}\right)^{\mathsf{T}}$ and $\boldsymbol{g}_k = \left(\boldsymbol{a}_{G,k}^{\mathsf{T}}, \boldsymbol{0}, \boldsymbol{0}\right)^{\mathsf{T}}$, where $\boldsymbol{1}_{b_\nu,k}$ denotes the Euclidean basis vector in $\mathbb{R}^{b_\nu}$ with all vanishing elements except the k-th component equal to 1, and $\boldsymbol{a}_{G,k}$ is the k-th column of $\boldsymbol{A}_G$;
- the constant vectors $\boldsymbol{q}_k \in \mathbb{R}^m$ collect the sets $\{\boldsymbol{q}_k\}_{k=1}^{b_d} = \{\boldsymbol{l}_k\}_{k=1}^{b_L} \cup \{\boldsymbol{c}_k\}_{k=1}^{b_C}$ individually defined as $\boldsymbol{l}_k = \left(\boldsymbol{0}, \boldsymbol{0}, \boldsymbol{1}_{b_L,k}^{\mathsf{T}}\right)^{\mathsf{T}}$ and $\boldsymbol{c}_k = \left(\boldsymbol{a}_{C,k}^{\mathsf{T}}, \boldsymbol{0}, \boldsymbol{0}\right)^{\mathsf{T}}$, where $\boldsymbol{a}_{C,k}$ is the k-th column of $\boldsymbol{A}_C$;
- the constant matrix $\boldsymbol{\mathcal{G}}_0$ is defined as

$$\boldsymbol{\mathcal{G}}_0 = \begin{pmatrix} \boldsymbol{0} & \boldsymbol{A}_R & \boldsymbol{A}_L \\ -\boldsymbol{A}_R^{\mathsf{T}} & \boldsymbol{0} & \boldsymbol{0} \\ -\boldsymbol{A}_L^{\mathsf{T}} & \boldsymbol{0} & \boldsymbol{0} \end{pmatrix}. \tag{7}$$

3.2 Parameterization for Uncertainty Quantification

For the uncertainty quantification problem to be well posed, we assume that the circuit is well defined and uniquely solvable for all parameter configurations, i.e., $\exists s \in \mathbb{C}$ for which $\det(\boldsymbol{\mathcal{G}}(\boldsymbol{\theta}) + s\boldsymbol{\mathcal{C}}(\boldsymbol{\zeta})) \neq 0$. Equivalently, the pencil $(\boldsymbol{\mathcal{G}}, \boldsymbol{\mathcal{C}})$ is regular for any $\boldsymbol{\theta}, \boldsymbol{\zeta}$. We further consider a nominal parameter configuration $\boldsymbol{\theta} = \bar{\boldsymbol{\theta}}$ and $\boldsymbol{\zeta} = \bar{\boldsymbol{\zeta}}$. For instance, this nominal configuration can be considered as the set of expected values of the circuit element values, assumed to be stochastic variables. The initial hypothesis also implies unique solvability for this nominal parameter configuration, which is the only assumption required by the following derivations.

We introduce the variable transformation

$$\boldsymbol{\theta} = \bar{\boldsymbol{\theta}} + \boldsymbol{\varepsilon}, \quad \boldsymbol{\zeta} = \bar{\boldsymbol{\zeta}} + \boldsymbol{\delta}, \tag{8}$$

where each element of vectors $\boldsymbol{\varepsilon}$ and $\boldsymbol{\delta}$ is a zero-mean stochastic variable, and we denote $\bar{\boldsymbol{\mathcal{G}}} = \boldsymbol{\mathcal{G}}(\bar{\boldsymbol{\theta}})$ and $\bar{\boldsymbol{\mathcal{C}}} = \boldsymbol{\mathcal{C}}(\bar{\boldsymbol{\zeta}})$. Due to linearity, (6) can now be written as

$$\boldsymbol{\mathcal{G}} = \boldsymbol{\mathcal{G}}(\boldsymbol{\varepsilon}) = \bar{\boldsymbol{\mathcal{G}}} + \sum_{k=1}^{b_a} (\boldsymbol{p}_k \boldsymbol{p}_k^\mathsf{T})\, \varepsilon_k, \quad \boldsymbol{\mathcal{C}} = \boldsymbol{\mathcal{C}}(\boldsymbol{\delta}) = \bar{\boldsymbol{\mathcal{C}}} + \sum_{k=1}^{b_d} (\boldsymbol{q}_k \boldsymbol{q}_k^\mathsf{T})\, \delta_k. \tag{9}$$

We see that both the static ($\boldsymbol{\mathcal{G}}$) and the dynamic ($\boldsymbol{\mathcal{C}}$) MNA matrices are expressed as a finite sum of rank-one updates with respect to the nominal circuit formulation. Each rank-one update pertains to a single individual stochastic circuit element. The corresponding constant rank-one matrices $\boldsymbol{p}_k \boldsymbol{p}_k^\mathsf{T}$ and $\boldsymbol{q}_k \boldsymbol{q}_k^\mathsf{T}$ are recognized as the standard MNA stamps of the various circuit elements.

Let us now consider the Laplace-domain solution of (4), which in the present case corresponds to the impedance matrix of the considered P-port element and reads

$$\boldsymbol{Z}(s;\boldsymbol{\xi}) = \boldsymbol{\mathcal{B}}^\mathsf{T} \left[\boldsymbol{\mathcal{G}}(\boldsymbol{\varepsilon}) + s\,\boldsymbol{\mathcal{C}}(\boldsymbol{\delta})\right]^{-1} \boldsymbol{\mathcal{B}} = \frac{\mathsf{N}(s;\boldsymbol{\xi})}{\mathsf{D}(s;\boldsymbol{\xi})}, \tag{10}$$

where we have collected all stochastic parameters in a single vector $\boldsymbol{\xi}$ having elements $\{\xi_k\}_{k=1}^d = \{\varepsilon_k\}_{k=1}^{b_a} \cup \{\delta_k\}_{k=1}^{b_d}$, with $d = b_a + b_d$ being the total number of uncertain circuit elements, as previously defined in Section 2. In (10), the scalar denominator $\mathsf{D}(s;\boldsymbol{\xi})$ coincides with the determinant of the MNA matrix $\boldsymbol{\mathcal{Y}}(s;\boldsymbol{\xi}) = \boldsymbol{\mathcal{G}}(\boldsymbol{\varepsilon}) + s\,\boldsymbol{\mathcal{C}}(\boldsymbol{\delta})$, whereas each element of the numerator $\mathsf{N}(s;\boldsymbol{\xi})$ is a linear combination of the determinants of the submatrices (minors) obtained from $\boldsymbol{\mathcal{Y}}(s;\boldsymbol{\xi})$ by deleting one row and one column.

We now provide an explicit characterization of the numerator and denominator of (10). To this end, we collect all stochastic parameters in a diagonal matrix

$$\boldsymbol{\Xi} = \mathrm{diag}(\xi_1, \ldots, \xi_d), \tag{11}$$

which we use to cast the MNA matrix in the compact form, by restating (9) as

$$\boldsymbol{\mathcal{Y}}(s;\boldsymbol{\xi}) = \bar{\boldsymbol{\mathcal{Y}}}(s) + \boldsymbol{U}\boldsymbol{\Xi}\boldsymbol{S}(s). \tag{12}$$

The matrix $\bar{\boldsymbol{\mathcal{Y}}}(s) = \bar{\boldsymbol{\mathcal{G}}} + s\,\bar{\boldsymbol{\mathcal{C}}}$ corresponds to the nominal configuration, and

$$\boldsymbol{U} = \begin{pmatrix}\boldsymbol{P} \; \boldsymbol{Q}\end{pmatrix}, \quad \boldsymbol{S}(s) = \begin{pmatrix}\boldsymbol{P} \; s\boldsymbol{Q}\end{pmatrix}^\mathsf{T}, \tag{13}$$

where the constant matrices $\boldsymbol{P}$ and $\boldsymbol{Q}$ collect as columns all the vectors $\boldsymbol{p}_k$ and $\boldsymbol{q}_k$, respectively. From now on, we will omit the dependence on the Laplace variable s, since we are interested in the dependence on the stochastic variables $\boldsymbol{\xi}$.

We introduce two useful lemmas:

Lemma 1. *Given a square invertible matrix $\boldsymbol{X}$ and two matrices $\boldsymbol{U}, \boldsymbol{V}$ of compatible size, we have*

$$\det(\boldsymbol{X} + \boldsymbol{U}\boldsymbol{V}^\mathsf{T}) = \det(\boldsymbol{I} + \boldsymbol{V}^\mathsf{T}\boldsymbol{X}^{-1}\boldsymbol{U}) \cdot \det(\boldsymbol{X}).$$

The above Lemma 1 is known as *matrix determinant lemma*, see [6] for a proof.

Lemma 2. *Let a matrix $\boldsymbol{W} \in \mathbb{R}^{n,n}$ have elements in the form $W_{ij} = F_{ij} + \xi_i B_{ij}$, where F_{ij}, B_{ij} are constants for $i, j = 1, \ldots, n$, and ξ_i are independent parameters.*

Then,

$$\det(\boldsymbol{W}) = \sum_k \beta_k \prod_{\ell=1}^{n} \xi_\ell^{\alpha_{k\ell}}, \tag{14}$$

where $\alpha_{k\ell} \in \{0,1\}$ $\forall k,\ell$, and β_k are real constants.

Proof. We use an induction argument, noting that the statement is trivially verified for $n = 1$. Assuming that the statement holds for size $n-1$, we evaluate $\det(\boldsymbol{W})$ for size n, for which $\boldsymbol{W}$ reads

$$\boldsymbol{W} = \begin{pmatrix} F_{11} + \xi_1 B_{11} & F_{12} + \xi_1 F_{12} & \cdots & F_{1n} + \xi_1 B_{1n} \\ F_{21} + \xi_2 B_{21} & F_{22} + \xi_2 F_{22} & \cdots & F_{2n} + \xi_2 B_{2n} \\ \vdots & \vdots & \ddots & \vdots \\ F_{n1} + \xi_n B_{n1} & F_{n2} + \xi_n F_{n2} & \cdots & F_{nn} + \xi_n B_{nn} \end{pmatrix}.$$

Expanding $\det(\boldsymbol{W})$ using Laplace's formula along the first row, we get

$$\det(\boldsymbol{W}) = \sum_{j=1}^{n} (-1)^{1+j} (F_{1j} + \xi_1 B_{1j}) M_{1j}, \tag{15}$$

where M_{1j} is the determinant of the submatrix of size $n-1$ obtained by deleting row 1 and column j from $\boldsymbol{W}$. By the induction ansatz, we have

$$M_{1j} = \sum_k \beta_k \prod_{\ell=2}^{n} \xi_\ell^{\alpha_{k\ell}}, \quad \alpha_{k\ell} \in \{0,1\} \quad \forall k,\ell. \tag{16}$$

Inserting (16) into (15) leads to

$$\begin{aligned} \det(\boldsymbol{W}) &= \sum_{j=1}^{n} (-1)^{1+j} (F_{1j} + \xi_1 B_{1j}) \sum_k \beta_k \prod_{\ell=2}^{n} \xi_\ell^{\alpha_{k\ell}} \\ &= \sum_k \sum_{j=1}^{n} (-1)^{1+j} \left[F_{1j} \beta_k \prod_{\ell=2}^{n} \xi_\ell^{\alpha_{k\ell}} + B_{1j} \beta_k \xi_1 \prod_{\ell=2}^{n} \xi_\ell^{\alpha_{k\ell}} \right] = \sum_k \hat{\beta}_k \prod_{\ell=1}^{n} \xi_\ell^{\alpha_{k\ell}}, \end{aligned}$$

where $\alpha_{k\ell} \in \{0,1\}$ for $\ell = 1, \ldots, n$ and $\forall k$, and $\hat{\beta}_k$ are constants. □

We are now ready to calculate the denominator $\mathsf{D}(s;\boldsymbol{\xi})$ in (10) as

$$\mathsf{D} = \det\left(\bar{\boldsymbol{\mathcal{Y}}} + \boldsymbol{U}\boldsymbol{\Xi}\boldsymbol{S}\right). \tag{17}$$

Applying Lemma 1 with $\boldsymbol{V}^{\mathsf{T}} = \boldsymbol{\Xi}\boldsymbol{S}$ and $\boldsymbol{X} = \bar{\boldsymbol{\mathcal{Y}}}$, we have

$$\mathsf{D} = \det\left(\boldsymbol{I} + \boldsymbol{\Xi}\boldsymbol{B}\right) \cdot \det\left(\bar{\boldsymbol{\mathcal{Y}}}\right), \tag{18}$$

where both $\boldsymbol{B} = \boldsymbol{S}\bar{\boldsymbol{\mathcal{Y}}}^{-1}\boldsymbol{U}$ and $\det\left(\bar{\boldsymbol{\mathcal{Y}}}\right)$ depend only on s and are thus constant with respect to the stochastic parameters $\boldsymbol{\xi}$. We have

$$\boldsymbol{I}+\boldsymbol{\Xi}\boldsymbol{B}=\begin{pmatrix}1+\xi_1 B_{11} & \xi_1 B_{12} & \cdots & \xi_1 B_{1n}\\ \xi_2 B_{21} & 1+\xi_2 B_{22} & \cdots & \xi_2 B_{2n}\\ \vdots & \vdots & \ddots & \vdots\\ \xi_n B_{n1} & \xi_n B_{n2} & \cdots & 1+\xi_n B_{nn}\end{pmatrix}.$$

This matrix verifies the conditions of Lemma 2 with $\boldsymbol{F}=\boldsymbol{I}$. Therefore

$$\det\left(\boldsymbol{I}+\boldsymbol{\Xi}\boldsymbol{B}\right)=\sum_k \beta_k \prod_{\ell=1}^{n} \xi_\ell^{\alpha_{k\ell}} \tag{19}$$

with $\alpha_{k\ell}\in\{0,1\}$ for all k,ℓ, which in turn implies that

$$\mathsf{D}(s;\boldsymbol{\xi})=\sum_k \mathsf{d}_k(s)\prod_{\ell=1}^{n}\xi_\ell^{\alpha_{k\ell}},\quad \alpha_{k\ell}\in\{0,1\}\quad \forall k,\ell. \tag{20}$$

Due to the lumped nature of the system under consideration, the coefficients $\mathsf{d}_k(s)$ are polynomials in s of degree up to the dynamic order N of the circuit.

The same arguments used for the denominator $\mathsf{D}(s;\boldsymbol{\xi})$ can be seamlessly adopted to show that also the elements of the numerator matrix $\mathbf{N}(s;\boldsymbol{\xi})$ in (10) have the same structural dependence on frequency s and parameters $\boldsymbol{\xi}$. Therefore, we conclude that any element (i,j) of the impedance matrix $\boldsymbol{Z}(s;\boldsymbol{\xi})$ has the following structure

$$Z_{ij}(s;\boldsymbol{\xi})=\frac{\sum_{k=0}^{N_{ij}} a_{k;ij}(\boldsymbol{\xi})s^k}{\sum_{k=0}^{N} b_k(\boldsymbol{\xi})s^k}, \tag{21}$$

where all numerator and denominator coefficients $a_{k;ij}(\boldsymbol{\xi})$ and $b_k(\boldsymbol{\xi})$ have a *multi-linear* dependence in the stochastic parameters, i.e., they are multivariate polynomials in which each element of $\boldsymbol{\xi}$ appears with up to order one. In conclusion, any impedance element is a rational function of any stochastic parameter ξ_i with both numerator and denominator degrees that cannot exceed one.

Based on the above result, the RPC model (1) is exact for linear lumped circuits, provided that the polynomial basis functions φ_ℓ are multi-linear. This is readily achieved by adopting a tensor-product truncation of order one [3]. By extension, the model turns out to be more accurate also for distributed circuits and electromagnetic systems, albeit with higher-degree approximations, as was effectively and empirically demonstrated based on a number of application examples in [3].

4 An Illustrative Example

We consider the filter of Fig. 1 (left), which is designed to exhibit both a band- and a high-pass behavior. All 9 circuit elements are uncertain, with inductances and capacitances having independent Gaussian variations with a 20% standard deviation around the nominal values indicated in the schematic.

The right panel in Fig. 1 shows the variability of the insertion loss of the filter. The gray lines are a subset of random samples from a reference Monte Carlo (MC) simulation with 10000 runs, whereas the solid blue line is the standard deviation of the MC samples. The dashed red and green lines are the standard deviations obtained with a conventional PCE having a maximum total degree of three, and with a tensor-product RPC model having a maximum degree of one, respectively. The conventional model has 220 terms in its single PCE, and the corresponding coefficients are calculated by means of an ordinary least square regression [2]. The RPC model has a total of 1023 terms (512 in the numerator and 511 in the denominator), and the coefficients are calculated with an iterative linearized least-square regression [3]. In both cases, we use a number of regression samples that is twice the number of unknowns.

As expected, the RPC provides an exact model, and the result is therefore consistent with the reference MC curve. This is further confirmed by the mean squared deviation of the two models from the MC samples, which is 3.8574×10^{-2} and 2.6264×10^{-10} for the conventional PCE and the RPC model, respectively.

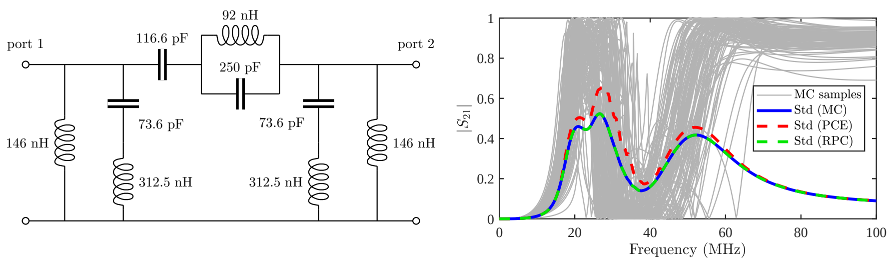

Fig. 1 Left: filter schematic. Right: variability of the insertion loss of the filter. Gray lines: MC samples; solid blue, dashed red, and dashed green lines: standard deviation obtained with MC, conventional PCE, and proposed RPC methods, respectively.

5 Conclusions

This work presented a formal derivation that any frequency-domain transfer function defined on linear lumped circuits is a rational function with multi-linear dependence on the circuit element values. This results provides a rigorous motivation for using a Rational Polynomial Chaos (RPC) model for the uncertainty quantification of the frequency-domain responses of electrical circuits, and more generally of electromagnetic systems. Our findings are illustrated based on a lumped filter example.

While a first-order tensor-product truncation provides an exact model for lumped circuits, a more compact total-degree truncation (possibly of higher order) can be used to improve the efficiency, especially for applications in which the exactness no longer holds. This is the case, for example, of distributed, electromagnetic, and/or photonic systems. We are also currently investigating a compression strategy, based on principal component analysis, that avoids having to optimize the model coefficients separately for each frequency.

References

1. Xiu, D.: Fast numerical methods for stochastic computations: a review. Commun. Computational Physics, **5**(2–4), 242–272 (2009)
2. Kaintura, A., Dhaene, T., Spina, D.: Review of polynomial chaos-based methods for uncertainty quantification in modern integrated circuits. Electronics, **7**(3), 30:1–21 (2018)
3. Manfredi, P., Grivet-Talocia, S.: Rational polynomial chaos expansions for the stochastic macromodeling of network responses. IEEE Trans. Circuits Syst. I, Reg. Papers, **67**(1), 225–234 (2020)
4. Vlach, J., Singhal, K.: Computer Methods for Circuit Analysis and Design. Wiley, New York (1983)
5. Ho, C.-W., Ruehli, A., Brennan, P.: The modified nodal approach to network analysis. IEEE Trans. Circuits Syst., **22**(6), 504–509 (1975)
6. Harville, D.A.: Matrix Algebra From a Statistician's Perspective. Springer-Verlag, New York (1997)